NANOSYSTEMS: PHYSICS, CHEMISTRY, MATHEMATICS, 2016, 7 (4), P. 604–608

Dynamic study of bismuth telluride quantum dot assisted titanium oxide for efficient photoelectrochemical performance

Pallavi B. Patil, Vijay V. Kondalkar, Kishorkumar V. Khot, Chaitali S. Bagade, Rahul M. Mane, P. N. Bhosale*

Materials Research Laboratory, Department of Chemistry, Shivaji University, Kolhapur–416004, India

*p_n_bhosale@rediffmail.com

PACS 82.45 Mp **DOI 10.17586/2220-8054-2016-7-4-604-608**

The 3D TiO_2 microflowers, sensitized by Bi_2Te_3 nanoparticles, having novel architecture were generated employing a two-step synthetic strategy, including a hydrothermal process and a potentiostatic electrodeposition technique. The design and synthesis of quantum dots (QDs) for achieving high photoelectrochemical performance is an urgent need for high technology fields

Keywords: Bi_2Te_3 QDs assisted TiO_2, 1D nanorods, PEC.

Received: 30 January 2016

Revised: 6 May 2016

1. Introduction

Quantum dot-sensitized solar cells (QDSCs) have received much attention because they are promising candidates for low cost and large area photovoltaic applications. Semiconductor quantum dot-sensitized solar cells (QDSSCs) have the advantages of being low cost and a simple fabrication process. The most attractive property of a semiconductor quantum dot is its ability to promote the photoconversion efficiency above Shockley-Queisser limit. The low efficiency of QDSSCs is attributed to the relatively low photovoltage in the cell compared to DSSCs and to the recombination paths induced by the electronic properties of the interfaces formed at TiO_2-QD-electrolyte triple junction [1]. Secondly, it is difficult to incorporate QDs into a TiO_2 mesoporous matrix to obtain a well-covered QD monolayer on the inner surface of the TiO_2 electrode. Other possible reasons include QD-electrolyte interfaces [2], electron loss occurring through charge recombination at the TiO_2-electrolyte interface [3]. To achieve higher performance photovoltaic solar cells, morphologies and structures of anode materials are also widely investigated [4]. In general, mesoporous TiO_2 nanoparticles are the most frequently used photoanodes in DSSCs and QDSSCs, due to their high internal surface area for sufficient sensitizer anchoring [5]. Unfortunately, mesoporous TiO_2 nanoparticles have some disadvantages, such as charge collection rate due to surface states and grain boundaries existing in the pathway of nanoparticles, which can lead to many unexpected trapping and de-trapping, and thus, inferior light scattering [6]. In this study, we successfully synthesized vertically aligned TiO_2 nanorods sensitized by Bi_2Te_3 nanoparticles. The photoelectrochemical performance of TiO_2 is greatly improved by sensitization of TiO_2 by Bi_2Te_3 nanoparticles [7]. The sensitization of TiO_2 by Bi_2Te_3 nanoparticles leads to a separation of the charge carriers. The charge separation leads to a reduction in the overall recombination in the solar cells and the enhancement of photogenerated carrier collection.

2. Method

First, TiO_2 can be prepared by our previously-reported hydrothermal method [7]. In detail 0.04 M TTIP was added in the solution containing 3M HCl and ethylene glycol stirred for some time. The clear transparent solution then poured into a Teflon-lined stainless steel autoclave maintained at 160°C for 2 h. The electrodeposition of Bi_2Te_3 nanoparticles on TiO_2 thin films was accomplished in a three electrode cell configuration containing aqueous solutions of 7 mM Bi $(NO_3)_3$ and 10 mM Te in 1M HNO_3. The deposition was carried out at -0.8 V vs Ag/AgCl. In this, TiO_2 nanorods act as working electrode, platinum as counter electrode and Ag/AgCl as reference electrode. The deposition time was fixed at 30 min. and the depositions were carried out at room temperature. In order to control the size of Bi_2Te_3 nanoparticles and prevent large particle formation, PVA was used as structure directing agent.

3. Results and discussion

3.1. Optical absorption spectra of Bi_2T_3 loaded TiO_2

The light absorption properties of Bi_2Te_3-loaded TiO_2 thin was evaluated using the UV-visible spectrophotometer (Shimadzu UV-1800 Japan). Figure 1 shows the Tauc plot of Bi_2Te_3 loaded TiO_2 thin films. The band gap energy of composite can be expressed by the Tauc relation. It is well known that there are fundamental optical transitions, namely directly-allowed (n=1/2) and indirectly-allowed (n=2) transition. It is also noteworthy that the band gap energy of Bi_2Te_3 loaded TiO_2 heterostructures was found to be 2.1 eV, indicating the optical absorption of the hybrid nanostructure has been extended from the UV region to the visible region.

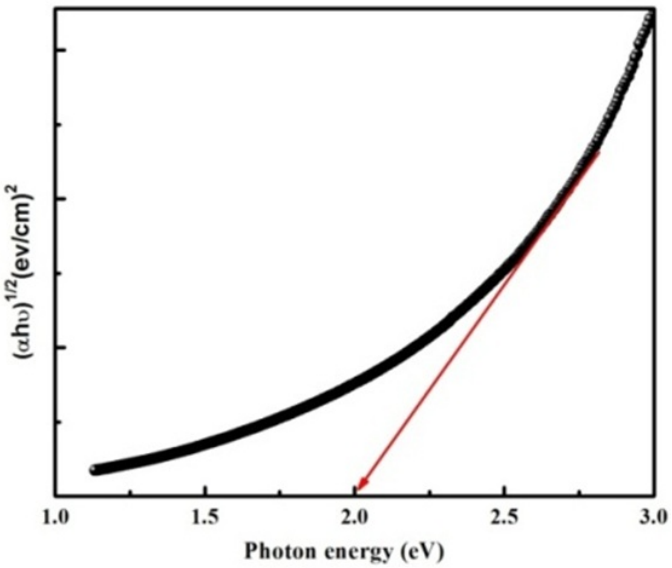

FIG. 1. Optical absorption spectra of Bi_2Te_3 loaded TiO_2 thin film

3.2. X-ray diffraction (XRD) pattern of Bi_2T_3 loaded TiO_2 thin film

The strong characteristic diffraction peak appeared at around 27.70° corresponds to (110) peak associated with rutile phase of TiO_2 (Space Group: P42/ mnm, JCPDS: 00-001-0562) (Rigaku, D/MAX Ultima III XRD spectrometer (Japan)). Furthermore, it should be noted that diffraction peak appearing at 27.67° corresponds to the (015) plane of Rhombohedral Bi_2Te_3 (JCPDS: 15-0863 space group R-3m) shown in Fig. 2. Due to overlap between (110) plane of TiO_2 and (015) plane of Bi_2Te_3, it is difficult to distinguish these two peaks in the XRD pattern. While the other peaks appeared at 2θ 27.70°, 36.22°, 41.35°, 54.58°, 56.97° and 65.54°, corresponding to the (110), (101), (111), (211), (220) and (221) crystal plane of tetragonal TiO_2 and 27.67°, 37.86°, 62.91° and 69.91° corresponding to the (015), (1010), (0213) and (0216) crystal planes of rhombohedral Bi_2Te_3.

It was found that the diffraction peak of the resulting deposit confirms the successful loading of Bi_2Te_3 nanoparticles on TiO_2. The crystallite size of the material was calculated by using Debye Scherrer formula, given in equation 1:

$$D = \frac{0.94\lambda}{\beta \cos\theta}, \tag{1}$$

where D is crystallite size, θ is Peak position of X-ray diffraction, β is Full Width at Half Maxima (FWHM) in radian, λ is Wavelength of X-ray used (0.154 nm). The XRD parameters are summarized in Table 1.

TABLE 1. XRD parameters.

Sample	Crystallite Size (D) (nm)	Microstrain(ε) 10^{-3} (lines m^{-2})	Dislocation density (δ)$\times 10^{-3}$ (lines^{-2} m^{-4})
Bi_2Te_3 loaded TiO_2	16.78	20156	3.5515

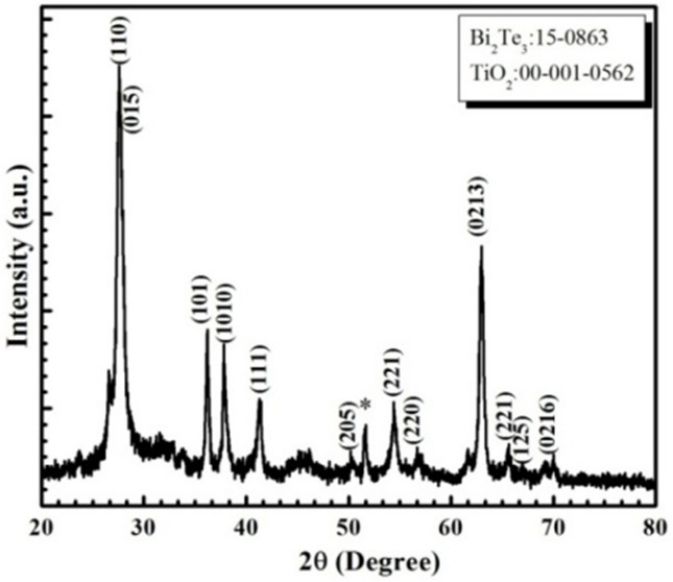

FIG. 2. X-ray diffraction pattern of Bi_2Te_3 loaded TiO_2 thin film

3.3. Field Emission Scanning Electron Microscopy (FESEM) of Bi_2T_3 loaded TiO_2 thin film

The morphological analysis of the synthesized material was carried out using field emission scanning electron microscopy (FESEM) (Hitachi, S-4700). Fig. 3 shows the low and high magnification field emission scanning electron microscopy (FESEM) images. The FESEM image shows that entire surface of FTO substrate is covered with well-aligned TiO_2 nanorods coated with Bi_2Te_3 nanoparticles. From the higher magnification of such nanorod arrays, the average diameter of the TiO_2 nanorod is 95–110 nm.

After Bi_2Te_3 quantum dot loading, the TiO_2 nanorods become rough, which means that the QDs have been successfully deposited on the surface of the TiO_2 nanorods after potentiostatic electrodeposition. The vertical alignment of the TiO_2 nanorods is beneficial for the improvement in the charge transfer of the solar cells. Such deep penetration of Bi_2Te_3 nanoparticles into the TiO_2 nanorods improves the charge separation and reduces recombination rate, which is beneficial for the photoelectrochemical performance of the solar cell.

3.4. Compositional analysis Bi_2Te_3 loaded TiO_2 thin film

Qualitative and quantitative analysis of the prepared Bi_2Te_3 loaded TiO_2 was carried out using energy dispersive X-ray spectroscopy (EDS).

The EDS spectrum confirms the presence of titanium, oxygen, bismuth and tellurium in prepared Bi_2Te_3 loaded TiO_2 thin film. From Figure 4, it is readily seen that the peaks at 4.5, 0.5, 2.4 and 3.7 keV confirm the presence of Ti, O, Bi and Te respectively in the Bi_2Te_3-loaded TiO_2 film.

3.5. Photoelectrochemical performance (PEC)

The typical J-V characteristic curve of Bi_2Te_3-loaded TiO_2 thin film was determined. The photoelectrochemical performance of the Bi_2Te_3-loaded TiO_2 thin film was carried out using a two electrode cell configuration (AUTOLAB PGSTAT100 FRA 32 potentiostat). In order to evaluate the photoelectrochemical performance, the Bi_2Te_3-loaded TiO_2 thin film acts as a photoanode, graphite as counter electrode with 0.5 polysulfide electrolyte. The cell configuration is as follows: Glass/ FTO/ Bi_2Te_3 loaded TiO_2/ 0.5M Polysulphide/G .

The photoelectrochemical performance i.e. fill factor (FF) and overall light to electric energy conversion efficiency (%) was calculated by equation (2) and (3):

$$FF = \frac{V_{max} J_{max}}{V_{oc} J_{sc}} \tag{2}$$

$$\eta_{\%} = \frac{V_{oc} J_{sc}}{P_{in} \times FF \times 100,} \tag{3}$$

where V_{oc} is open circuit voltage, J_{sc} is short circuit current, V_{max} is maximum voltage, J_{max} is maximum current, FF is the fill factor and P_{in} is the intensity of the incident light.

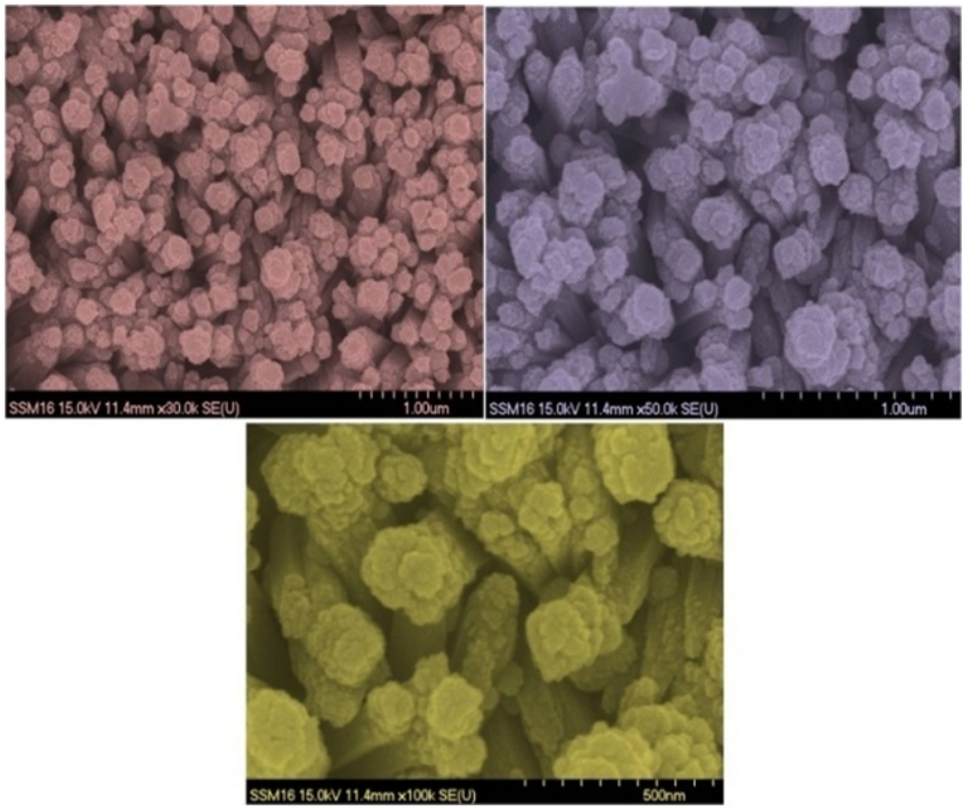

FIG. 3. Field emission scanning electron microscopy images of Bi_2Te_3 loaded TiO_2 thin film

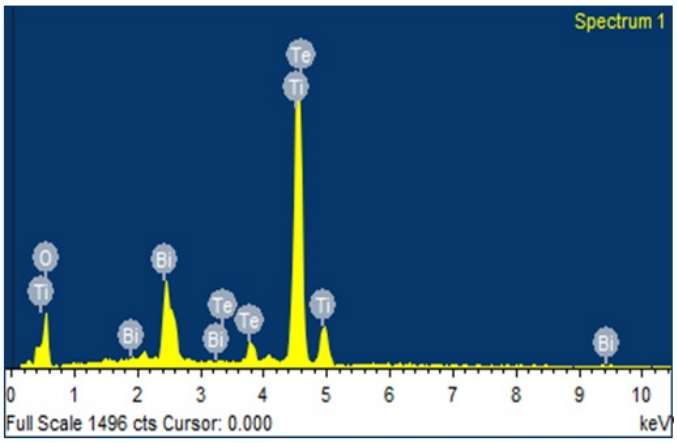

FIG. 4. EDS spectrum of Bi_2Te_3 loaded TiO_2 thin film

The detailed photovoltaic parameters are summarized in Table 2. The Bi_2Te_3-loaded TiO_2 thin film shows 0.026% photoconversion efficiency.

TABLE 2. Photoelectrochemical solar cell parameters of Bi_2Te_3 loaded TiO_2 thin film

Electrode	V_{oc} (mV)	J_{sc} (μA/cm^2)	R_s (Ω)	R_{sh} (Ω)	$\eta_{\%}$
Bi_2Te_3 loaded TiO_2	397.03	61	2660	4762	0.026

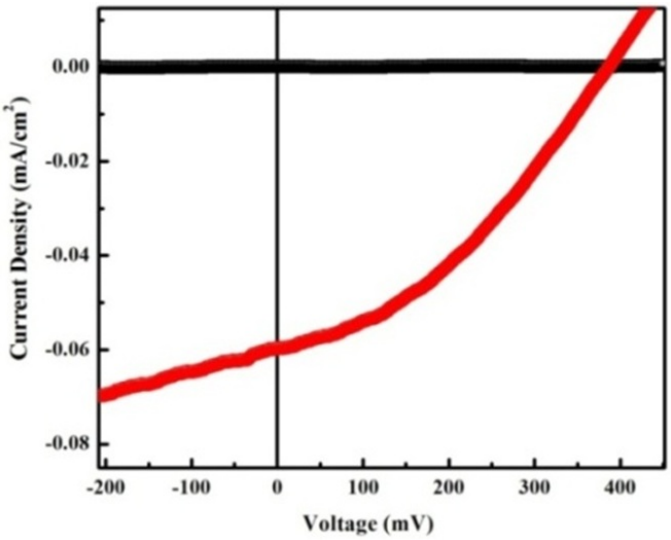

FIG. 5. J-V characteristic curve of Bi_2Te_3 loaded TiO_2 thin film

4. Conclusion

In summary, a Bi_2Te_3-loaded TiO_2 thin film was successfully prepared by a two-step synthetic strategy. 1D nanorods provided a unidirectional transport path for efficient charge, leading to high photoelectrochemical performance. Therefore, this novel combinatorial Bi_2Te_3 loaded TiO_2 thin film shows 0.026% photoconversion efficiency.

References

[1] Sero I., Gimenez S., Santiago F., Gomez R, Shen Q., Toyoda T., Bisquert J. Recombination in Quantum Dot Sensitized Solar Cells, *Acc. Chem. Res.*, 2009, **42**, P. 1848–1857.

[2] Diguna L., Murakami M., Sato A., Kumagai Y., Ishihara T., Kobayashi N., Shen Q., Toyoda T. Highly efficient CdS/CdSe-sensitized solar cells controlled by the structural properties of compact porous TiO_2 photoelectrodes. *J. Appl. Phys.*, 2008, **103**, P. 084304–084308.

[3] Lee Y., Chang C. Efficient polysulfide electrolyte for CdS quantum dot-sensitized solar cells. *J. Power Sources*, 2008, **185**, P. 584–588.

[4] Wu W., Xu Y., Su C., Kuang D. Ultra-long anatase TiO_2 nanowire arrays with multi-layered configuration on FTO glass for high-efficiency dye-sensitized solar cells. *Energy Environ. Sci.*, 2014, **7**, P. 644–649.

[5] Shiu J., Lan C., Chang Y., Wu H., Huang W., Diau Eric W. Size-Controlled Anatase Titania Single Crystals with Octahedron-like Morphology for Dye-Sensitized Solar Cells. *ACS Nano*, 2012, **6**, P. 10862–10873.

[6] Du J., Qi J., Wang D., Tang Z., Facile synthesis of Au@TiO_2 core-shell hollow spheres for dye-sensitized solar cells with remarkably improved efficiency. *Energy Environ. Sci.*, 2012, **5**, P. 6914–6918.

[7] Patil P., Mali S., Kondalkar V., Mane R., Patil P., Hong C., Bhosale P. Bismuth Telluride quantum dot assisted Titanium Oxide microflowers for efficient photoelectrochemical performance. *Mater. Lett.*, 2015, **159**, P. 177–181.

[8] Patil P., Mali S., Kondalkar V., Pawar N., Khot K., Hong C., Patil P., Bhosale P. Single step hydrothermal synthesis of hierarchical TiO_2 microflowers with radially assembled nanorods for enhanced photovoltaic performance. *RSC Adv.*, 2014, **4**, P. 47278–47286.